PHYSICAL REVIEW B **95**, 220501(R) (2017)

Pressure-induced bulk superconductivity in a layered transition-metal dichalcogenide 1*T*-tantalum selenium

Bosen Wang,[1,2,*] Yu Liu,[3] Kento Ishigaki,[1] Kazuyuki Matsubayashi,[1,4] Jinguang Cheng,[2] Wenjian Lu,[3] Yuping Sun,[3,5,6] and Yoshiya Uwatoko[1]

[1]*Institute for Solid State Physics, University of Tokyo, Kashiwanoha 5-1-5, Kashiwa, Chiba 277-8581, Japan*
[2]*Beijing National Laboratory for Condensed Matter Physics and Institute of Physics, Chinese Academy of Sciences, Beijing 100190, China*
[3]*Key Laboratory of Materials Physics, Institute of Solid State Physics, Chinese Academy of Sciences, Hefei 230031, China*
[4]*Department of Engineering Science, University of Electro-Communications, Chofu, Tokyo 182-8585, Japan*
[5]*High Magnetic Field Laboratory, Chinese Academy of Sciences, Hefei 230031, China*
[6]*Collaborative Innovation Center of Advanced Microstructures, Nanjing University, Nanjing 210093, China*

(Received 19 January 2017; revised manuscript received 12 May 2017; published 9 June 2017)

We report pressure-driven superconductivity (SC) in the vicinity of a commensurate charge-density wave (CCDW) in transition-metal dichalcogenides (TMDs) 1*T*-$TaSe_2$ by simultaneous resistivity and ac susceptibility. The superconducting phase enters at 4.5 GPa and bulk SC emerges along with the collapse of the CCDW phase at a critical pressure $P_c \sim 6.5$ GPa. Higher than P_c, the superconducting transition temperature (T_c) keeps increasing linearly, without a dome-shaped superconducting diagram in our pressure range. T_c reaches ~5.3 K at 15 GPa, which is the highest among all 1*T*-TMDs. A comprehensive analysis shows that electronic correlations of the CCDW phase open energy gaps, which prohibit Cooper pairing, while the superconducting channels and CCDW domain wall coexist in three dimensions above P_c. The evolutions of the Fermi surface and the softening of phonon modes under pressure are proposed to explain the monotonic increase of T_c. The findings reveal the interplay of CCDW and SC in 1*T*-$TaSe_2$ by a clean method, viz., high pressure, and shed light on the underlying superconducting mechanism in the relevant systems.

DOI: 10.1103/PhysRevB.95.220501

Charge-density waves (CDWs) and superconductivity (SC) are the basic low-energy collective excitations in condensed matter physics. When a CDW is formed, the periodic electron density modulations and the anisotropic energy gaps at the Fermi surface generate multiple commensurate electronic orders, either competing or cooperative [1–4]. Extensive effort has been devoted to the resultant electronic phase diagrams by controlling external stimulations to reveal the intrinsic physics [2–4]. For example, layered transition-metal dichalcogenides (TMDs) have been studied continuously for nearly 50 years [2,5], but the key factors concerning the CDW mechanism and the interplay of CDW and SC are far from clear, as they strongly rest with the crystal dimensionality, band structures, and tuning parameters [2–6].

In TMDs, melted CDWs versus external parameters (e.g., pressure, doping, thickness, electric field) often exhibit diverse superconducting phase diagrams [2–4,6–12]. In one case, the superconducting transition temperature (T_c) assumes a domelike shape close to the collapsed CDW in 2*H*-MX_2 (M = Ta, Mo, Nb; X = S, Se) [2,8,11,12], 1*T*-$TiSe_2$ [3,4,10], etc., while in other cases, T_c changes insensitively [6,13] and/or increases monotonously without domes [14]. In former, the superconducting dome resembles that of an unconventional SC neighboring quantum critical point (QCP) [15]. Thus, one scenario is proposed that the CDW fluctuation glues superconducting pairs [4] since CDW and SC jointly originate from Fermi surface instabilities and electron-phonon coupling, which was supported by Raman scattering studies [16] and theoretical calculations [17]. However, an opposite scenario is argued that CDW is weakly connected to SC (e.g., 1*T*-TaS_2) in 1*T*-TMDs, [7] and the dome-shaped superconducting diagram is far from a CDW QCP (e.g., 1*T*-$TiSe_2$) [18], which agrees with the evidence of a conventional single-gapped *s*-wave SC by analyzing the heat capacity and thermal properties [19,20]. Additionally, the superconducting diagram and the coexisting model of CDW and SC depend on tuning routes experimentally even from the same starting point (e.g., 1*T*-$TiSe_2$) [3,4]. Some argue that the CDW structure transits into SC collectively, and CDW and SC coexist on a macroscopic scale in real space [13], while others support the notion that insulating CDW domain walls coexist with superconducting interdomains [6,9,10,21]. It implies that the SCs are distinct in superconducting diagrams generated by different tuning parameters [3,4], and a coexisting model of CDW and SC is essential to understand the key factors of the superconducting mechanism [6,9,14]. Thus, further studies are valuable to figure out the existing pictures of CDW and SC, and to reveal their underlying physics.

1*T*-$TaSe_2$, with a higher commensurate (CCDW) than incommensurate (ICCDW) transition temperature ~473 K [5,9,22] and a larger unit-cell volume compared to isostructural 1*T*-$TiSe_2$, 1*T*-TaS_2, and several intercalated compounds [1,3–6], has attracted our attention as a starting point to explore SC and reveal the interplay of CDW instability and SC by pressure. At ambient pressure, 1*T*-$TaSe_2$ adopts a trigonal $P\bar{3}m1$ symmetry with a $\sqrt{13} \times \sqrt{13}$ Ta atom superstructure, which is shaped as a Star-of-David cluster [5,22,23]. In theory, 1*T*-$TaSe_2$ and 1*T*-TaS_2 possess similar band structures, opening Mott energy gaps in the Ta-5*d* bands

*bswang@iphy.ac.cn

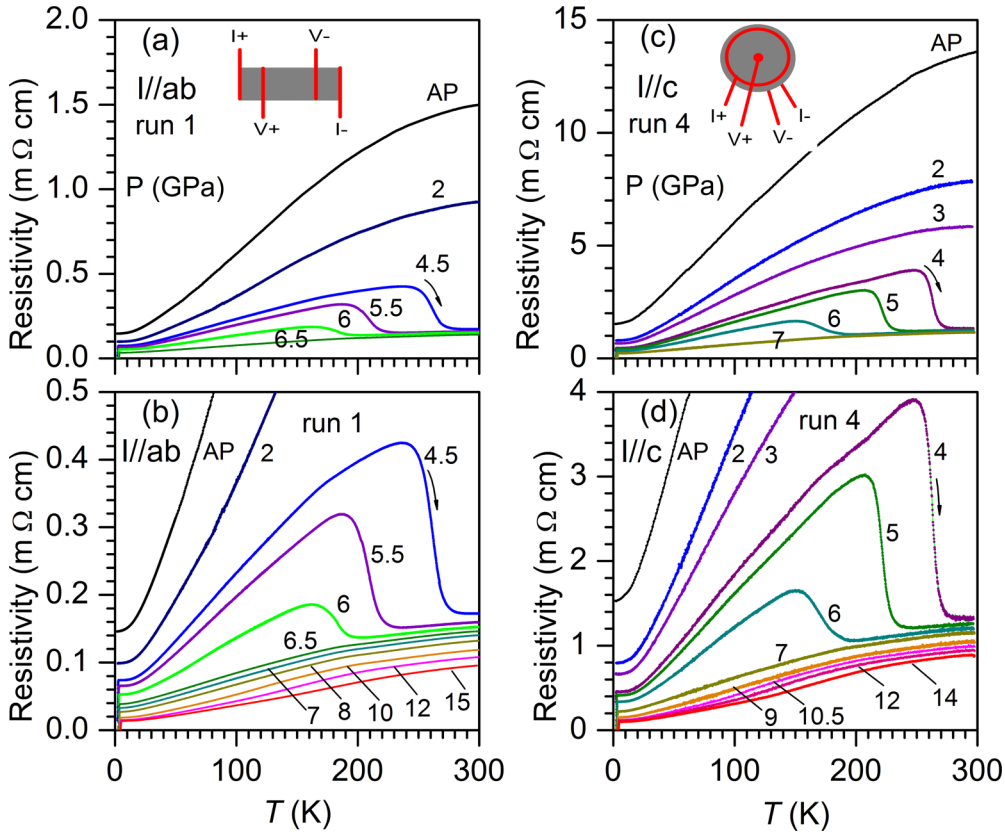

FIG. 1. Temperature dependence of resistivity $\rho(T)$ under various pressures to 15 GPa with the current parallel to (a) the ab plane and (c) the c axis; enlargement of $\rho(T)$ in (b) and (d).

owing to strong electronic localizations or correlations, against SC [24,25]. But the Fermi surfaces of the former are distinctive, containing a flat pancake-shaped area centered at the point Γ and a surrounding cylindrical electronic surface [26,27]. It implies that its band structure has three-dimensional (3D) characteristics dissimilar to two-dimensional (2D) crystals, which gives rise to speculation as to the origin of CDW in $1T$-$TaSe_2$ [21]. Two experimental indications reveal its complex electronic structures, namely, the anisotropic magnetoresistance effect and the transformation from a surface Mott insulator to a metal at 200 K in $1T$-$TaSe_2$ [28,29]. Additionally, it has been predicted theoretically that CCDW in $1T$-$TaSe_2$ is stable up to ∼30 GPa [21], which is six times higher than that of $1T$-TaS_2 (∼5 GPa) [6], and equivalent substitutions or "chemical pressures" in the Se/S site do not destroy the CCDW and the nearly commensurate CDW (NCCDW) [30]. These encourage us to explore the nature of $1T$-$TaSe_2$ in a clear and efficient way, viz., via high pressure. In this Rapid Communication, the electric transport and ac susceptibility of $1T$-$TaSe_2$ were investigated in a cubic anvil pressure cell [31]. Pressure-induced bulk SC was discovered and T_c increased with a parabolalike dependence reaching ∼5.3 K at 15 GPa, which is the highest among $1T$-TMDs [3,4,6,10,30].

Single-crystal $1T$-$TaSe_2$ was grown by chemical vapor transport using iodine as the transport agent; details of the processes are reported elsewhere [5,9,30]. Single-crystal x-ray diffraction was preformed to verify the phase purity. Lattice parameters are identical as before with a space group of $P\bar{3}m1$ (No. 164) [30]. High-pressure experiments were performed in a cubic anvil cell, which generate hydrostatic pressure conditions owing to the multiple anvil geometry, with a preheated MgO cube as the gasket and glycerin as the pressure transmitting medium [31,32]. Resistivity was measured using the four-probe method with the measuring current (I) parallel to the ab plane ($I \parallel ab$) (run 1, run 2) and the c axis ($I \parallel c$) (run 3, run 4). The sketch maps are shown in Figs. 1(a) and 1(c) for $I \parallel ab$ and $I \parallel c$, respectively .The room-temperature anisotropic resistivity is ∼5−10, depending on the samples, which is about half of the reports with out-of-plane resistivity using a dual-probe system [33]. The ratio is two orders smaller in magnitude compared to $1T$-TaS_2, implying considerable hybridized couplings of the Se-Ta-Se interlayers. ac susceptibility was collected at a frequency of 307 Hz under a small modulation magnetic field parallel to the ab plane. Cryogenic experiments were performed on a ^{4}He refrigerated cryostat.

Figure 1 shows the temperature dependence of resistivity $\rho(T)$ under various pressures up to 15 GPa. At ambient pressure, the CCDW-ICCDW transition in $1T$-$TaSe_2$ occurs at ∼473 K and opens an energy band gap ∼150 meV owing to the electron condensations [5,22,30,34]. This transformation is marked by a sharp jump in resistivity [4,22,30], and its transition temperature (T_{CCDW}) was determined by the maximum of $d\rho/dT$. In Figs. 1(a) and 1(b), as the pressure increases, the in-plane resistivity initially decreases and the CCDW-ICCDW transition is shifted down to ∼260 K at

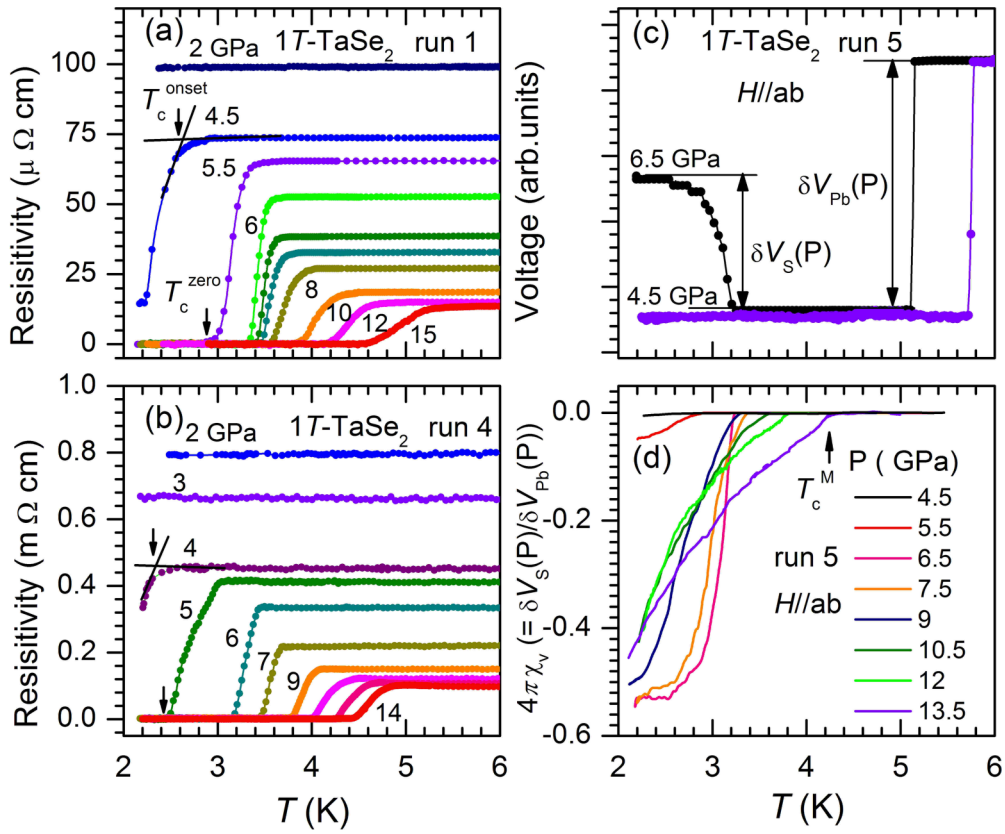

FIG. 2. Low-temperature $\rho(T)$ along (a) the ab plane and (b) the c axis. (c) ac susceptibility of $1T$-$TaSe_2$ and the reference Pb at 4.5 and 6.5 GPa using homemade pickup coils; the superconducting shield fraction was obtained compared with Pb. (d) Temperature-dependent susceptibility under various pressures; the arrows indicate the superconducting transition temperature T_c^M.

4.5 GPa, the CCDW-ICCDW transition broadens, and when the pressure is higher than 6.5 GPa, no detectable jump in resistivity was seen, which is evidence of a collapsed CCDW phase; when further increasing the pressure to 15 GPa, the magnitude of resistivity decreases nearly one order compared to ambient pressure. Figures 1(c) and 1(d) show the out-of-plane resistivity under various pressures: It displays an analogous pressure dependence as an the in-plane resistivity and the CCDW-ICCDW transition disappears around 7 GPa. Moreover, whether it is the ab plane or the c axis, clear thermal hysteresis of the CCDW-ICCDW transition occurs upon cooling/warming processes, indicating its first order as in other TMDs [6,11,14].

In Figs. 2(a) and 2(b), low-temperature $\rho(T)$ was shown in 2–6 K. At 4.5 GPa, $\rho(T)$ starts to drop due to the appearance of a superconducting phase combined with the following diamagnetic signals. The onset of the superconducting state (T_c^{onset}) is ~2.6 K, determined by the intersection of the linear parts of $\rho(T)$. Up to 5.5 GPa, a zero-resistivity state is reached and the superconducting transition temperature (T_c^{zero}) is ~2.9 K. With increasing pressure to 15 GPa, both T_c^{onset} and T_c^{zero} continue increasing. In Fig. 2(b), $\rho(T)$ starts to decrease at 4 GPa with $T_c^{\text{onset}} \sim 2.3$ K, and reaches zero at 5 GPa with $T_c^{\text{zero}} \sim 2.5$ K; then T_c^{onset} and T_c^{zero} increase monotonously. The results are plotted in Figs. 3(a), 3(b), and 3(d) and are not dependent on the runs. By fittings, it gives pressure coefficients ~0.200(5) and ~0.148(3) K/GPa for T_c^{onset} and T_c^{zero}, respectively. We note that T_c^{onset} (T_c^{zero}) reach ~5.3 K(4.6 K) at 15 GPa, which is the highest among $1T$-TMDs [3,4,6,10,30]. For example, in Cu_xTiSe_2, the maximum $T_c^{\text{onset}} \sim 4.2$ K for $x \sim 0.08$ [3]; without a zero resistivity state in other cases, $T_c^{\text{onset}} \sim 1.8$ K in $1T$-$TiSe_2$ [4], $T_c^{\text{onset}} \sim 5$ K in $1T$-TaS_2 [6], and $T_c^{\text{onset}} \sim 3.5$ K in $1T-TaSSe$ [30], etc.

The ac susceptibility provides substantial evidence for bulk SC and is essential for understanding the coexisting CDW and SC. As described in Fig. 2(c), susceptibility was collected by using homemade pickup coils with the magnetic field parallel to the ab plane of $1T$-$TaSe_2$. The superconducting shield fraction $4\pi\chi_v(2\,\text{K})$ was estimated by referring to Pb, and the transition temperatures T_c^M are plotted in Figs. 2(d), 3(d), and 3(f). In perfect agreement with the electrical transport, the diamagnetic signal is nearly zero at 4.5 GPa and starts to increase, which is evidence of pressure-induced SC in $1T$-$TaSe_2$. As above, a zero-resistivity state appears at 5.5 GPa; however, $4\pi\chi_v(2\,K)$ is only ~5% at 5.5 GPa, and the CCDW-ICCDW transition is retained at as high as 200 K; up to 6.5 GPa, $4\pi\chi_v(2\,\text{K})$ jumps to ~56%, and remains constant as the pressure increases further. Such a large diamagnetic response in susceptibility precludes the possibility of impurity phases, indicating that pressure-induced SC is the bulk source in $1T$-$TaSe_2$. We note that CCDW and SC coexist at a narrow pressure interval of 5–6.5 GPa in $1T$-$TaSe_2$. In conjunction with previous reports [6,9,10,21], a reasonable explanation is that superconducting channels form in real space and coexist with CCDW at 5–6.5 GPa.

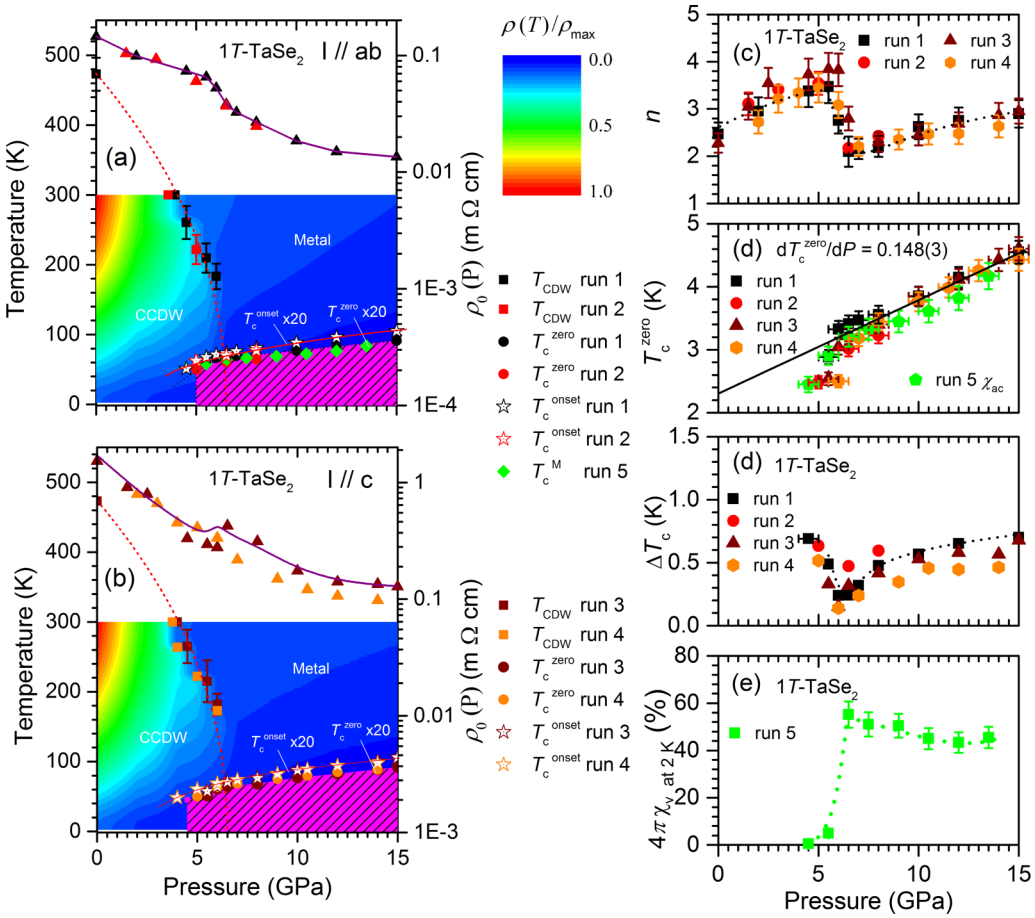

FIG. 3. (a), (b) T-P diagram and the colors describe the evolution of resistivity; the residual resistivity ρ_0 is estimated by fitting $\rho = \rho_0 + AT^n$ up to 20 K. The dashed red line, the red line, and the triangle points represent the trend of the CDW transition temperature, the onset of superconductivity, and the estimated residual resistivity (right-hand side); the value of $\rho^{\max}$ is defined as the resistivity of ρ_{ab} and ρ_c at 300 K and ambient pressure as 1.498 and 13.598 mΩ cm for $I \parallel ab$ and $I \parallel c$, respectively. The parameters as a function of pressure: (c) exponent n, (d) T_c^{zero} and T_c^{M}, (e) ΔT_c (defined as $T_c^{\text{onset}} - T_c^{\text{zero}}$), (f) $4\pi\chi_v$(2 K); the black line in (d) is the linear fitting and the lines across the data points in (c), (e), and (f) indicate the trends.

A T-P phase diagram of CCDW and SC is plotted in Figs. 3(a) and 3(b). Under pressure, T_{CCDW} decreases more rapidly when approaching P_c, similar to the QCP of the order phases [15,35]. The pressure evolution of T_{CCDW} is well fitted by the mean-field quantum fluctuation model as $T_{\text{CCDW}} = 473.9\ \text{K}(1 - P/P_c)^{\beta}$: The critical pressure P_c and the parameter β are 6.55(2) GPa and 0.466(2), respectively; The fitting results determine the critical pressure as 6.55(2) GPa where the CCDW totally disappears. The β value is half that of $1T$-TaS_2 ($\beta \sim 1$) [6,13], close to that of orthorhombic o-TaS_3($\beta \sim 0.5$) [36], both contrary to the usual behavior in conventional CDW materials [34]. Moreover, it is abnormal that $P_c \sim 6.5$ GPa is close to ~5 GPa in $1T$-TaS_2 experimentally [6], which is five times smaller in magnitude than that of theoretical predictions (~30 GPa) [21]. Such a differentiation is probably associated with the inappropriate model, lattice parameters, or other neglected factors such as the lattice potential. Considering that the CCDW-ICCDW transition is not strongly dependent on crystal anisotropy, the hybridization of CCDW orbitals along the c axis cannot be avoided and indicates that the CCDW-ICCDW transition occurs in three-dimensional (3D) crystals, which is consistent with previous studies on the Fermi structure [21,26,27]. On this basis, the coexistence of CCDW and SC can be in a 3D scale [21]. Or, more clearly, it means that the coexistence of superconducting pairing and the CCDW energy gap is simultaneously along the ab plane and the c axis. This behavior is abnormal and much different from other TMD compounds where the CCDW transition is almost two dimensional, as reported previously.

To correlate the diagram and the critical fluctuations or low-energy excitations, the normal-state $\rho(T)$ above T_c was fitted by the empirical formula of $\rho = \rho_0 + AT^n$, where ρ_0 represents the residual resistivity, and the coefficient A and the exponent n are related to the inelastic electron scatterings. In Figs. 3(a) and 3(b), ρ_0 decreases rapidly, except for a maximum at P_c, where the A value gets a maximum. The exponent n was estimated by fitting the temperature range from T_c up to 20 K: It initially increases slightly to ~3.5 ± 0.2 at 5.5 GPa, decreases to a minimum ~2.2 ± 0.1 at 6 GPa, and then increases to ~3.0 at 15 GPa. Unlike the empirical value for the electron-electron (electron-phonon) scatterings $n = 2(5)$, the decrease of n is unusual [5]. In general, the exponent n is associated with energy bands, disorders, crystal dimensionality, etc. Disorder

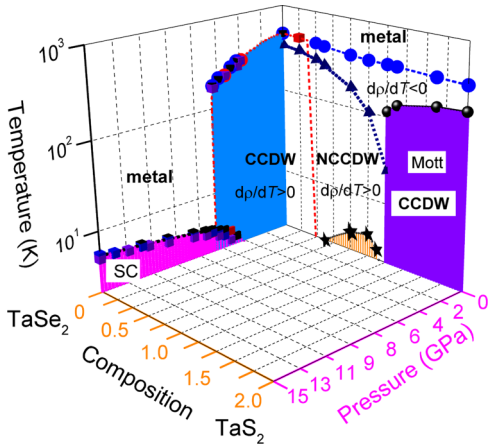

FIG. 4. Phase diagram of 1T-$TaSe_2$ in temperature, pressure, and composition. Here, the $d\rho/dT$ is the differential coefficient of resistivity. The red dashed line separates the CCDW and NCCDW and the triangle symbols divide the negative and positive $d\rho/dT$. The data at ambient pressure were provided by Liu as in Ref. [30].

is avoided under pressure and crystal anisotropy seems not to be as sensitive. In 1T-$TiSe_2$, a sizable suppression of n ($n = 3$ at ambient pressure to $n \sim 2.6$ at 2–4 GPa) near P_c was thought to be evidence of critical fluctuations [3,4]. In Cu_xZrTe_3, the intercalation caused a decrease from $n \sim 2.98$ in $ZrTe_3$ to $n \sim 2.7$ in $Cu_{0.05}ZrTe_3$, and it was attributed to the electron-electron umklapp process in theory [37]. Otherwise, phonon-assisted s-d interband scattering can explain $n \sim 3$ in $3DNb_3Ge$ [38]. Generally, for a CDW phase, the usual value of the exponent n is 3, as reported. However, with increasing pressure, the exponent of 1T-$TaSe_2$ first decreases near the critical pressure 6.5 GPa, and then recovers at higher pressure. Thus, it is reasonable to associate the n value with the electronic band gap, and the suppression of n can be seen as evidence for the enhanced critical fluctuations in 1T-$TaSe_2$ where the SC starts to appear. In Figs. 3(c)–3(f), ρ_0, T_c^{zero}, the superconducting transition width ΔT_c (defined as $T_c^{\text{onset}} - T_c^{\text{zero}}$), and $4\pi\chi_v(2\,\text{K})$ are summarized: T_c^{zero} increases with a positive pressure coefficient above 6.5 GPa; ΔT_c reaches a minimum of ~0.24 K at 6.5 GPa, while $4\pi\chi_v(2\,\text{K})$ gradually increases to ~56% at 6.5 GPa, and retains a constant. These characteristics indicate the interplay of CCDW and SC near P_c in 1T-$TaSe_2$.

Figure 4 presents an electronic diagram of 1T-$TaSe_2$ versus temperature, hydrostatic pressure, and composition [5,30]. Considering the pressure-induced scatterings are avoided, the contrastive studies on the diagrams versus pressure and doping can deepen our understanding: (1) "Chemical pressure" or S doping causes a transformation from a CCDW phase into a NCCDW phase, with T_{CCDW} reduced only ~20%(473−350 K), while CCDW completely collapses at 6.5 GPa; structurally, the volume of 1T-$TaSe_2$ contracts ~11.6% (~3.1% along the a and b axes and ~5.9% along the c axis) in 1T-$TaSe_{2-x}S_x$ [25,30], however, 1T-$TaSe_2$ shrinks ~5.6% in volume at 6.5 GPa compared to ambient pressure with a bulk modulus $B \sim 116.09$ GPa . It implies that the phase diagram of this system depends on tuning routes, and the impurity effect is critical to construct the 1T-$TaSe_{2-x}S_x$ diagram. (2) The narrow superconducting dome is submerged in the NCCDW phase and the superconducting shielding volume is small in 1T-$TaSe_{2-x}S_x$ [30]; under pressure, bulk SC is achieved above 6.5 GPa and T_c is enhanced as the pressure increases. Meanwhile, the optimal $T_c^{\max}$ is ~3.5 K in 1T-TaSSe, and lower than ~5.3 K in 1T-$TaSe_2$. All the above-mentioned characteristics imply that the superconducting properties of pressure-induced SC regions and the SC concerning the S/Se ratio at ambient pressure are distinct. Actually, it is clear that SC coexists with CCDW (above 300 K) in 1T-$TaSe_{2-x}S_x$ and no zero-resistivity state at ambient pressure while sharp and bulk SC phase transitions emerge near the CCDW phase boundary. Based on these results, the critical fluctuation near the CCDW phase boundary is believed to be an important exciton to superconducting pairs, as in other similar systems [2,3,15,35]. In a stable CCDW, the strong electronic correlations and Coulomb repulsions prevent superconducting pairings; when pressurized, the microregulations in the structure alter the electronic distributions, leading to a metastable CCDW and enhanced electron-phonon coupling, which is favorable to SC. Higher than P_c, the CCDW collapses and coexists with the superconducting channels in 3D scales [6,9,21].

Away from the CDW QCP, the disappearance of electronic correlations and/or critical fluctuations goes against SC; enhanced impurity scattering by doping also causes weakening of the electron-phonon coupling and a decrease of T_c [3,6,9]. However, in pressurized 1T-$TaSe_2$, T_c increases monotonously above 6.5 GPa. Several proposals may account for the elevated T_c: First, the softening of the phonon mode strengthens the electron-phonon coupling and is propitious to superconducting pairs in conventional SCs. [39,40]. Pressure-induced lattice deformation directly causes the instability of phonon vibration modes and an increase in the density of states at the Fermi level [39]. In previous studies, a softening of the phonon modes has been predicted in 1T-$TaSe_2$ [9,21] and is a response to positive pressure coefficients. Second, hybridizations of the phonon and exciton modes were proposed [40]. In Cu_xTiSe_2, the superconducting dome was interpreted by a phonon-mediated pairing mechanism. However, the pressure diagram of 1T-$TiSe_2$ cannot be explained by only using the simple model. The hybridization of phonon and exciton must be included, implying that 1T-$TiSe_2$ is one kind of elusive state in excitonic insulators or existing pseudogaps [41–43]. Considering their similar diagrams and bands, 1T-$TaSe_2$ is believed to be close to an excitonic insulator [4,41,43]. Under pressure, the excitonic insulator is melted and the superconducting state becomes robust with positive pressure coefficients. Third, the superconducting dome was argued to be away from the CCDW QCP in 1T-$TiSe_2$ [18], and ICCDW and SC coexist in the real space of 1T-Cu_xTiSe_2 and 1T-(Ti,Ta)Se_2 [13,25,41]. A further suppression of ICCDW may enhance SC. One such example is 1T-TaS_2, where light-induced metastable ICCDW phases were observed and the maximum of T_c is reached when all the ICCDWs are collapsed [44]. Integrated to the discussions, it increases the likelihood of different pressure-induced CDWs in 1T-$TaSe_2$ and a monotonic increase of T_c is seen as evidence of the competition between CDW and SC [21,22]. Additionally, the ICCDW phase disappears above 600 K in 1T-$TaSe_2$ [22,45] and its pressure dependence is critical. However, the transition cannot be detected in resistivity measurements. Thus, with

higher-pressure experiments, phonon spectra and theoretical calculations are required to understand the principle.

We acknowledge S. Nagasaki for technical assistance and thank Dr. J. Gouchi, Professor G. H. Cao, Dr. L. J. Li, and Dr. X. Luo for discussions. This work was supported by the National Key Research and Development Program of China (Grant No. 2016YFA0300404), the National Natural Science Foundation of China (Grants No. 11404342 and No. 11674326), and the Joint Funds of the National Natural Science Foundation and the Chinese Academy of Sciences' Large-Scale Scientific Facility (Grant No. U1232139). B.W. acknowledges the support of a JSPS fellowship for foreign researchers (Grant No. 15F15023). Y.U. is thankful for financial support from JSPS KAKENHI (Grant No. 15H03681).

B.W., Y.L., and K.I. contributed equally to this work.

[1] G. Grüner, Rev. Mod. Phys. **60**, 1129 (1988).
[2] H. Suderow, V. G.Tissen, J. P. Brison, J. L. Martinez, and S. Vieira, Phys. Rev. Lett. **95**, 117006 (2005).
[3] E. Morosan, H. W. Zandbergen, B. S. Dennis, J. W. G. Bos, Y. Onose, T. Klimczuk, A. P. Ramirez, N. P. Ong, and R. J. Cava, Nat. Phys. **2**, 544 (2006).
[4] A. F. Kusmartseva, B. Sipos, H. Berger, L. Forro, and E. Tutis, Phys. Rev. Lett. **103**, 236401 (2009).
[5] J. A. Wilson, F. J. Di Salvo, and S. Mahajan, Phys. Rev. Lett. **32**, 882 (1974).
[6] B. Sipos, A. Kusmartseva, A. Akrap, L. F. H. Berger, and E. Tutis, Nat. Mater. **7**, 960 (2008).
[7] Y. Yu, F. Y. Yang, X. F. Lu, Y. J. Yan, Y. H. Cho, L. G. Ma, X. H. Niu, S. Kim, Y. W. Son, D. L. Feng, S. Y. Li, S. W. Cheong, X. H. Chen, and Y. B. Zhang, Nat. Nanotechnol. **10**, 270 (2015).
[8] M. Yoshida, R. Suzuki, Y. Zhang, M. Nakano, and Y. Iwasa, Sci. Adv. **1**, e1500606 (2015).
[9] Y. Liu, D. F. Shao, L. J. Li, W. J. Lu, X. D. Zhu, P. Tong, R. C. Xiao, L. S. Ling, C. Y. Xi, L. Pi, H. F. Tian, H. X. Yang, J. Q. Li, W. H. Song, X. B. Zhu, and Y. P. Sun, Phys. Rev. B **94**, 045131 (2016).
[10] L. J. Li, E. C. T. Ofarrell, K. P. Loh, G. Eda, B. Ozyilmaz, and A. H. Castro Neto, Nature (London) **529**, 185 (2016).
[11] W. Shi, J. T. Ye, Y. Zhang, R. Suzuki, M. Yoshida, J. Miyazaki, N. Inoue, Y. Saito, and Y. Iwasa, Sci. Rep. **5**, 12534 (2015).
[12] D. C. Freitas, P. Rodière, M. R. Osorio, E. Navarro-Moratalla, N. M. Nemes, V. G. Tissen, L. Cario, E. Coronado, M. García-Hernández, S. Vieira, M. Núñez-Regueiro, and H. Suderow, Phys. Rev. B **93**, 184512 (2016).
[13] T. Ritschel, J. Trinckauf, G. Garbarino, M. Hanfland, M. v. Zimmermann, H. Berger, B. Buchner, and J. Geck, Phys. Rev. B **87**, 125135 (2013).
[14] R. Yomo, K. Yamaya, M. Abliz, M. Hedo, and Y. Uwatoko, Phys. Rev. B **71**, 132508 (2005).
[15] N. D. Mathur, F. M. Grosche, S. R. Julian, I. R. Walker, D. M. Freye, R. K. W. Haselwimmer, and G. G. Lonzarich, Nature (London) **394**, 39 (1998).
[16] H. Barath, M. Kim, J. F. Karpus, S. L. Cooper, P. Abbamonte, E. Fradkin, E. Morosan, and R. J. Cava, Phys. Rev. Lett. **100**, 106402 (2008).
[17] M. A. Rahimi and A. G. Moghaddam, Phys. Rev. B **95**, 104515 (2017).
[18] Y. I. Joe, X. M. Chen, P. Ghaemi, K. D. Finkelstein, G. A. de la Pena, Y. Gan, J. C. T. Lee, S. Yuan, J. Geck, G. J. MacDougall, T. C. Chiang, S. L. Cooper, E. Fradkin, and P. Abbamonte, Nat. Phys. **10**, 421 (2014).
[19] S. Y. Li, G. Wu, X. H. Chen, and L. Taillefer, Phys. Rev. Lett. **99**, 107001 (2007).
[20] J. Kačmarčík, Z. Pribulová, V. Pal'uchová, P. Szabó, P. Husaníková, G. Karapetrov, and P. Samuely, Phys. Rev. B **88**, 020507(R) (2013).
[21] Y. Z. Ge and A. Y. Liu, Phys. Rev. B **82**, 155133 (2010); A. Y. Liu, *ibid.* **79**, 220515(R) (2009).
[22] S. S. Sun, L. L. Wei, Z. W. Li, G. L. Cao, Y. Liu, W. J. Lu, Y. P. Sun, H. F. Tian, H. X. Yang, and J. Q. Li, Phys. Rev. B **92**, 224303 (2015).
[23] R. Brouwer and F. Jellinek, Physica B **99**, 51 (1980).
[24] K. Horiba, K. Ono, J. H. Oh, T. Kihara, S. Nakazono, M. Oshima, O. Shiino, H. W. Yeom, A. Kakizaki, and Y. Aiura, Phys. Rev. B **66**, 073106 (2002).
[25] R. Ang, Y. Miyata, E. Leki, K. Nakayama, T. Sato, Y. Liu, W. J. Lu, Y. P. Sun, and T. Takahashi, Phys. Rev. B **88**, 115145 (2013).
[26] R. Inada, Y. Onuki, and S. Tanuma, Physica B+C **99**, 188 (1980).
[27] A. M. Woolley and G. Wexler, J. Phys. C: Solid State Phys. **10**, 2601 (1977).
[28] P. D. Hambourger and F. J. Disalvo, Bull. Am. Phys. Soc. **23**, 245 (1978).
[29] S. Colonna, F. Ronci, A. Cricenti, L. Perfetti, H. Berger, and M. Grioni, Phys. Rev. Lett. **94**, 036405 (2005).
[30] Y. Liu, R. Ang, W. J. Li, W. H. Song, L. J. Li, and Y. P. Sun, Appl. Phys. Lett. **102**, 192602 (2013).
[31] N. Mori *et al.*, High Press. Res. **24**, 225 (2004).
[32] J.-G. Cheng, K. Matsubayashi, S. Nagasaki, A. Hisada, T. Hirayama, M. Hedo, H. Kagi, and Y. Uwatoko, Rev. Sci. Instrum. **85**, 093907 (2014).
[33] P. D. Hambourger and F. J. Disalvo, Physica B **99**, 173 (1980).
[34] P. Monceau, Adv. Phys. **61**, 325 (2012).
[35] M. Hashimoto, I. M. Vishik, R. H. He, T. P. Devereaux, and Z. X. Shen, Nat. Phys. **10**, 483 (2014).
[36] M. Monteverde, J. Lorenzana, P. Monceau, and M. Núñez-Regueiro, Phys. Rev. B **88**, 180504(R) (2013).
[37] X. D. Zhu, H. C. Lei, and C. Petrovic, Phys. Rev. Lett. **106**, 246404 (2011).
[38] D. W. Woodard and G. D. Cody, Phys. Rev. **136**, A166 (1964).
[39] W. L. McMillan, Phys. Rev. **167**, 331 (1968).
[40] L. R. Testardi, Rev. Mod. Phys. **47**, 637 (1975).
[41] M. Maschek, S. Rosenkranz, R. Heid, D. Zocco, A. H. Said, A. Alatas, G. Karapetrov, S. Zhu, J. van Wezel, and F. Weber, Phys. Rev. B **94**, 214507 (2016).
[42] K. W. Zhang, C. L. Yang, B. Lei, P. C. Lu, X. B. Li, Z. Y. Jia, Y. H. Song, J. Song, X. H. Chen, J. X. Li, and S. C. Li, arXiv:1611.10145.
[43] C. Monney, M. Puppin, C. W. Nicholson, M. Hoesch, R. T. Chapman, E. Springate, H. Berger, A. Magrez, C. Cacho, R. Ernstorfer, and M. Wolf, Phys. Rev. B **94**, 165165 (2016).
[44] T. T. Han, F. Zhou, C. D. Malliakas, P. M. Duxbury, S. D. Mahanti, M. G. Kanatzidis, and C. Y. Ruan, Sci. Adv. **1**, e1400173 (2015).
[45] R. Samnakay, D. Wickramaratne, T. P. Pope, R. K. Lake, T. T. Salguero, and A. A. Balandin, Nano Lett. **15**, 2965 (2015).